# Science Advances

AAAS

## Supplementary Materials for

## An anticancer drug suppresses the primary nucleation reaction that initiates the production of the toxic Aβ42 aggregates linked with Alzheimer's disease

Johnny Habchi, Paolo Arosio, Michele Perni, Ana Rita Costa, Maho Yagi-Utsumi, Priyanka Joshi, Sean Chia, Samuel I. A. Cohen, Martin B. D. Müller, Sara Linse, Ellen A. A. Nollen, Christopher M. Dobson, Tuomas P. J. Knowles, Michele Vendruscolo

**The PDF file includes:**

Fig. S1. Comparison of the effects of bexarotene and tramiprosate on Aβ42 aggregation.
Fig. S2. Quantitative evaluation of the effect of bexarotene on the rate constants of Aβ42 aggregation.
Fig. S3. HSQC spectra of $^{15}$N-Aβ42 in the absence and in the presence of fivefold excess of bexarotene.
Fig. S4. Interaction between $^{15}$N-Aβ42 and bexarotene.
Fig. S5. Effect of bexarotene on Aβ42 aggregation in *C. elegans*.
Fig. S6. Effect of DMSO on Aβ42 aggregation.
Fig. S7. Toxicity induced by bexarotene in SH-SY5Y human neuroblastoma cells.
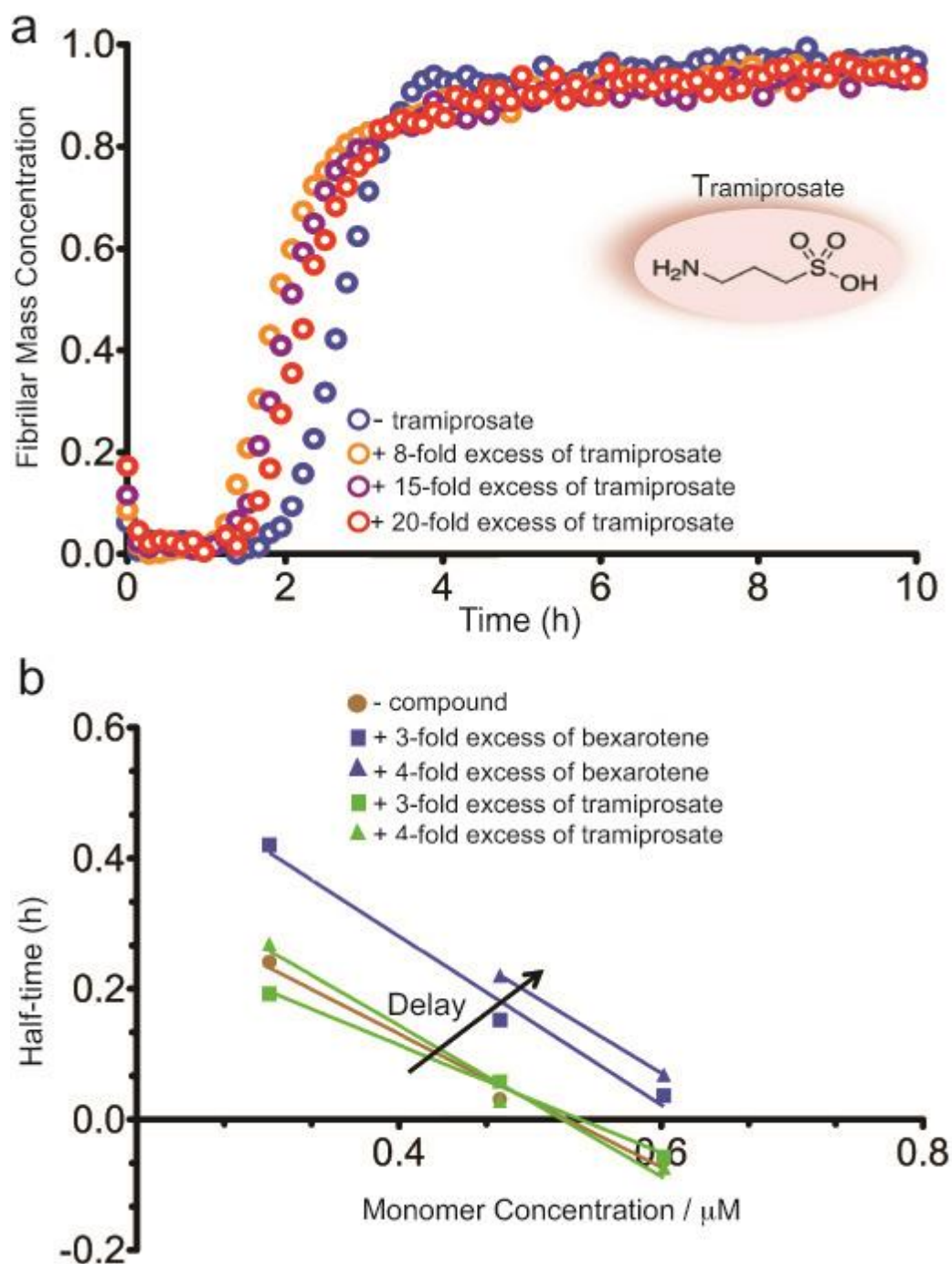
**Figure S1: Comparison of the effects of bexarotene and tramiprosate on Aβ42 aggregation. (a)** Kinetics profiles of the aggregation of 2 μM Aβ42 under quiescent conditions in the absence and in the presence of either 8-fold, or 15-fold or 20-fold excess of tramiprosate. **(b)** Average half-time as a function of the initial monomer concentration in the absence or the presence of either 3-fold or 4-fold excess of bexarotene or tramiprosate. Note that the delay in Aβ42 aggregation is observed only in the presence of bexarotene.
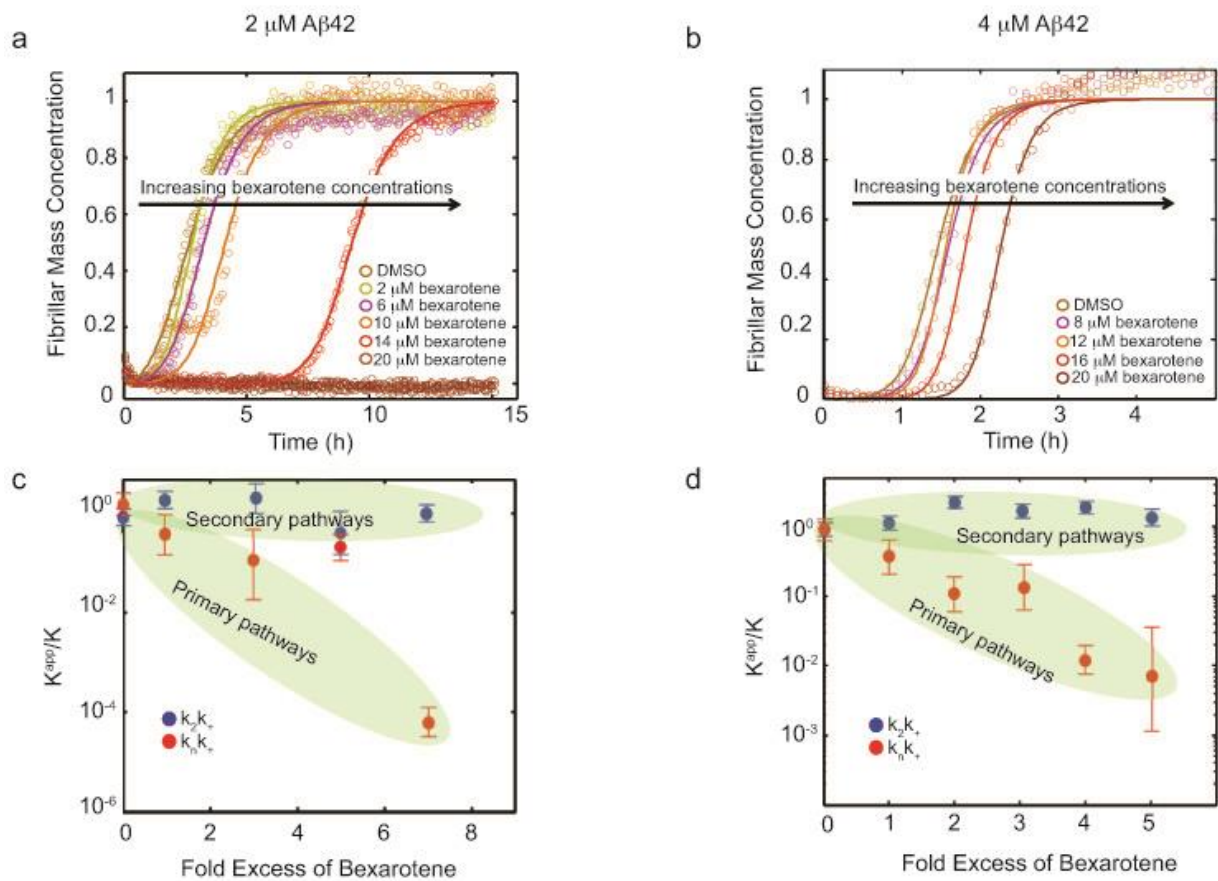
**Figure S2: Quantitative evaluation of the effect of bexarotene on the rate constants of Aβ42 aggregation.** Kinetic profiles of the aggregation of 2 μM **(a)** and 4 μM **(b)** Aβ42 in the absence or in the presence of increasing concentrations of bexarotene (represented by different colors). The global experimental profiles are well described by a kinetic model (represented by solid lines) that considers a specific inhibition of the primary nucleation rate constant, $k_n$. **(c, d)**, Plots of the evolution of the apparent reaction rate constants with increasing fold excesses of bexarotene ($k_n$ for primary nucleation, $k_+$ for elongation and $k_2$ for secondary nucleation). Note the significant decrease in primary pathways, $k_n k_+$, when compared to secondary pathways, $k_2 k_+$.
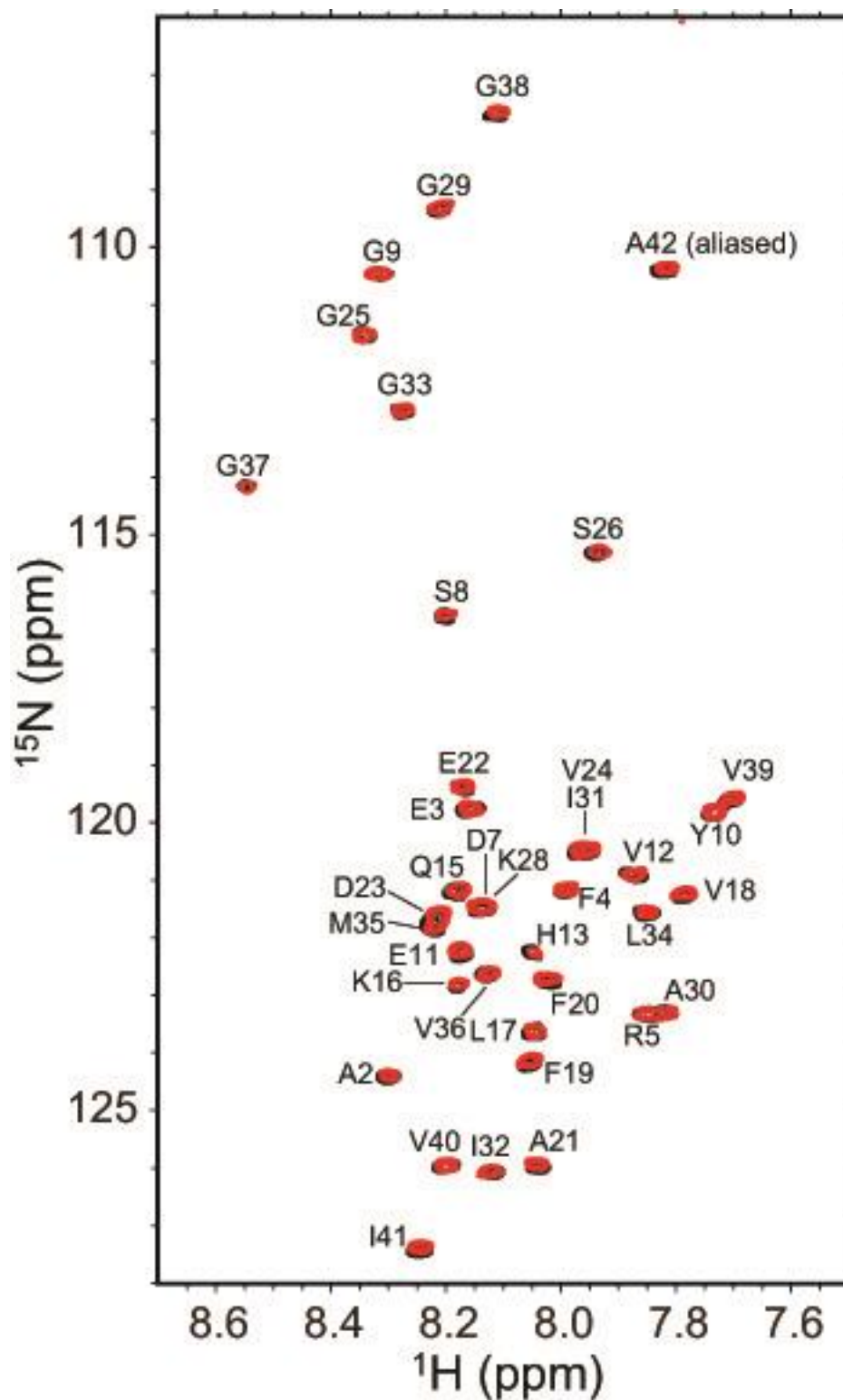
**Figure S3: HSQC spectra of $^{15}$N-A$\beta$42 in the absence and the presence of fivefold excess of bexarotene.** Superimposition of the $^1$H -$^{15}$N HSQC spectra of 25 $\mu$M monomeric $^{15}$N-A$\beta$42 in the absence (black) and in the presence of 5-fold excess of bexarotene (red). The spectra were obtained at a $^1$H frequency of 500 MHz and 278 K.
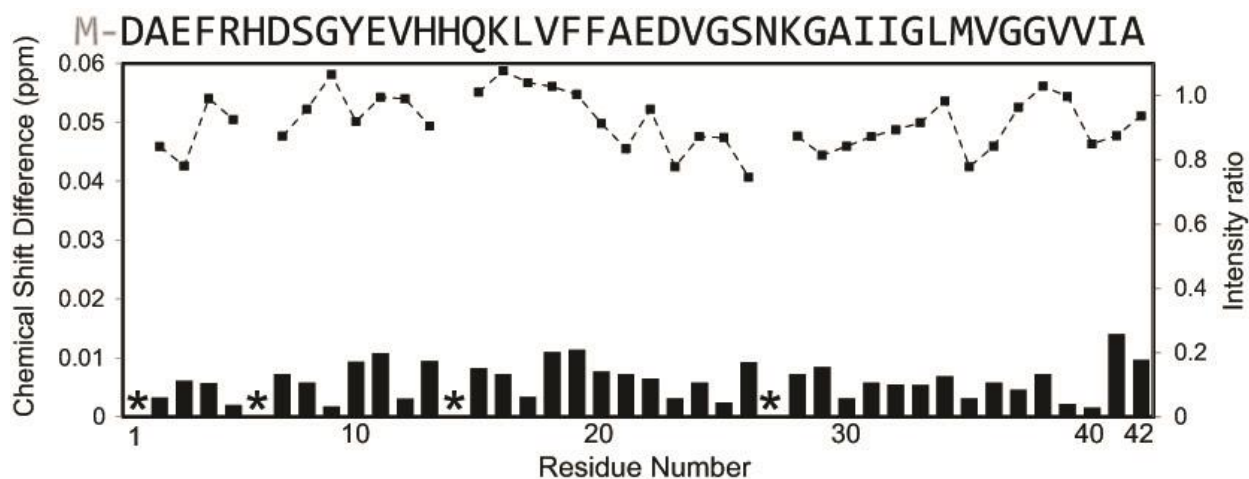
**Figure S4: Interaction between ^{15}N-Aβ42 and bexarotene.** Chemical shifts (bar graph) and normalized intensity (dotted line) of 25 μM monomeric ^{15}N-Aβ42 in the presence of 5-fold excess of bexarotene in 2.5% DMSO are similar to those observed for Aβ42 in the absence of bexarotene suggesting that persistent binding events are unlikely to occur.
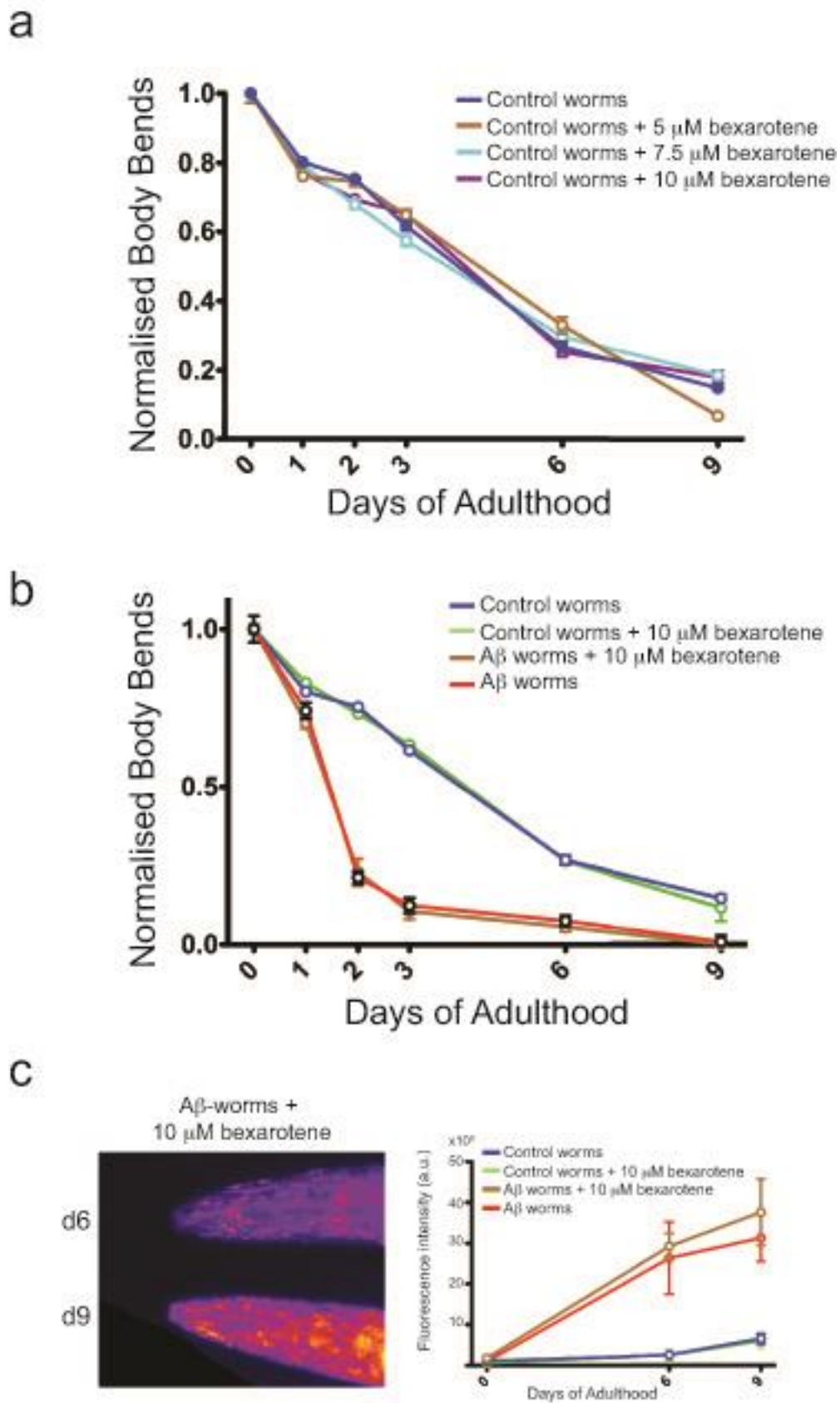
**Figure S5: Effect of bexarotene on Aβ42 aggregation in *C. elegans*.**
**(a)** Measurements of the effect of increasing concentrations of bexarotene ranging from

5 to 10 $\mu$M on the frequency of body bends of control models of *C. elegans.* Normalized values with respect to day 0 are shown. One experiment is shown as a representative of four independent experiments (n ≥ 111). Note the absence of effect of bexarotene at concentrations as high as 10 $\mu$M on the control worm model, thus supporting a specific A$\beta$-bexarotene interaction. **(b)** Effect of bexarotene at 10 $\mu$M concentration on the frequency of body bends given only at day 2 of the A$\beta$ and control-worm models. Data are shown for a single experiment but are representative of three independent experiments. Normalized values with respect to day 0 are shown. (**c**) Time course *in vivo* imaging and quantification of amyloid aggregates formed in A$\beta$ and control-worm models in the absence and in the presence of bexarotene at a concentration of 10 $\mu$M that was given only at day 2. Images of aggregates were taken *in vivo* with a Zeiss Axio Observer fluorescence microscope after staining with NIAD-4 as an amyloid-specific dye. Quantification of fluorescence intensity was performed using ImageJ software (see Methods). In all panels, error bars represent the SEM.
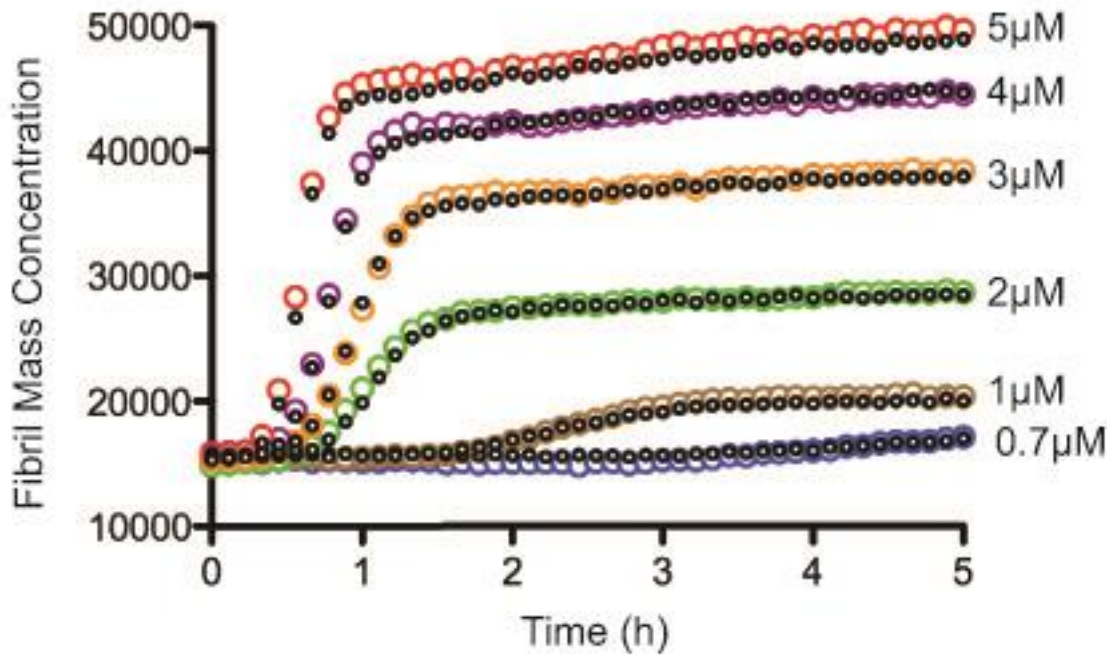
**Figure S6: Effect of DMSO on Aβ42 aggregation.** Superimposition of the kinetic profiles of Aβ42 aggregation at 6 initial monomer concentrations in the absence (shown in colors) or in the presence (shown in black) of 1% DMSO. The addition of 1% DMSO affects neither the slope nor the lag time of the aggregation of Aβ42.
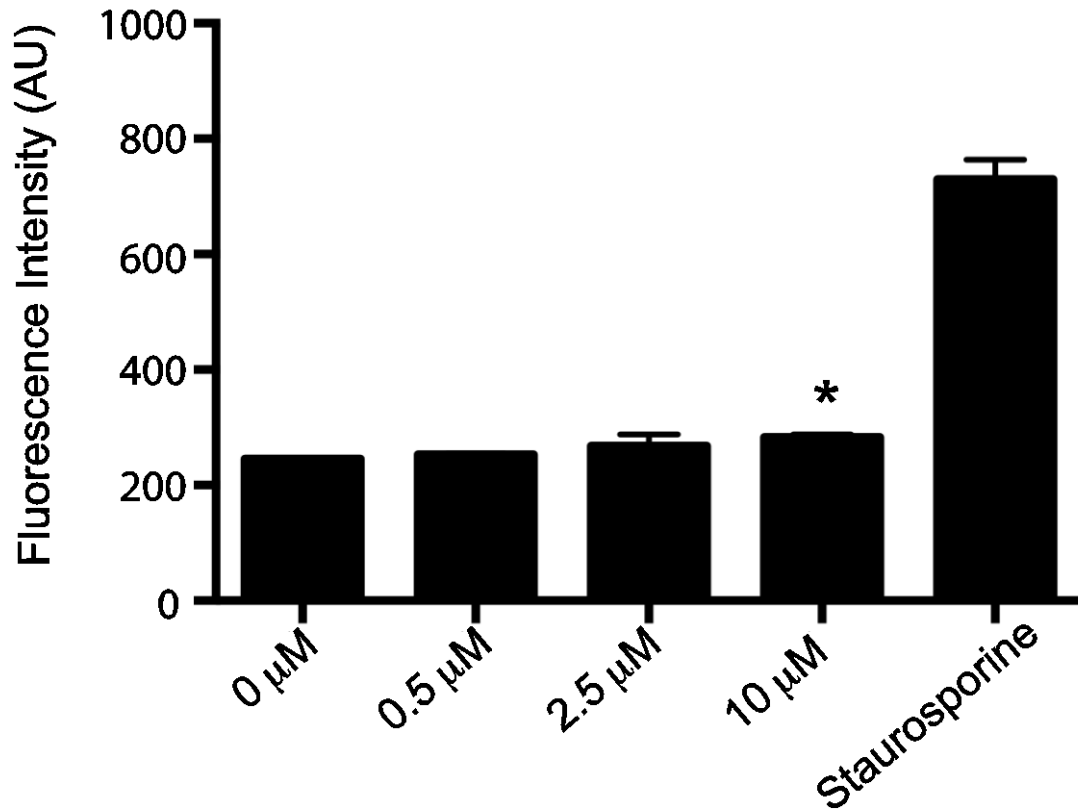
**Figure S7: Toxicity induced by bexarotene in SH-SY5Y human neuroblastoma cells.** No toxicity was detected for DMSO-solubilized (i.e. 1% DMSO final concentration) bexarotene in the concentration range of 1 $\mu$M to 10 $\mu$M. 10 $\mu$M (labeled with a star) is the concentration of bexarotene that was used in the toxicity assays.